

Parametric Instability of Axially Moving Media Subjected to Multifrequency Tension and Speed Fluctuations

R. G. Parker¹

Mem. ASME
e-mail: parker.242@osu.edu

Y. Lin

Graduate Student

Department of Mechanical Engineering,
The Ohio State University,
206 W. 18th Avenue,
Columbus, OH 43210-1107

This work investigates the stability of axially moving media subjected to parametric excitation resulting from tension and translation speed oscillations. Each of these excitation sources has spectral content with multiple frequencies and arbitrary phases. Stability boundaries for primary parametric instabilities, secondary instabilities, and combination instabilities are determined analytically through second-order perturbation. The classical result that primary instability occurs when one of the excitation frequencies is close to twice a natural frequency changes as a result of multiple excitation frequencies. Unusual interactions occur for the practically important case of simultaneous primary and secondary instabilities. While sum type combination instabilities occur, no difference type instabilities are detected. The nonlinear limit cycle amplitude that occurs under primary instability is derived using the method of multiple scales. [DOI: 10.1115/1.1343914]

Introduction

The transverse vibration of axially moving materials subjected to parametric excitations has received considerable attention from many researchers. Most studies have addressed the stability under parametric excitation with a single frequency component. Practical systems, however, are subjected to multifrequency excitations that may significantly impact the dynamic behavior. In vehicle serpentine belt drives, for example, the engine drives a crankshaft pulley that powers a single belt, which in turn supplies power to multiple automotive accessories. Engine firing pulses cause belt translation speed fluctuations. Additionally, these engine firing pulses, in combination with dynamic accessory torques, excite pulley rotational vibrations that lead to tension oscillations in the individual belt spans. The speed and tension fluctuations both parametrically excite the belt spans. The speed oscillations have spectral content related to harmonics of the engine speed, and the tension oscillations have multifrequency spectral content associated with the engine speed and dynamic accessory load frequencies.

This study investigates the stability of parametrically excited, moving media subjected to dynamic tension and speed fluctuations with arbitrary spectral content. A discretization/perturbation method yields the excitation frequency-amplitude parameter plane boundaries separating stable and unstable regions for the single mode primary and secondary resonances and the combination resonances for any two modes. These boundaries are determined analytically in closed form through second-order perturbation. Nonlinear limit cycles that occur in the parametric resonance regions are determined analytically and numerically.

This work builds on that of Mockensturm et al. [1], who determined closed-form analytical expressions for all primary and the first sum type combination resonance regions of a moving string with tension fluctuation. Similarly, Pakdemirli and Ulsoy [2] de-

termined stability boundaries for the moving string with speed fluctuation. Both of these analyses are limited to monofrequency parametric excitation and first-order approximation. They do not address secondary resonances. The present work shows unique and practically important behaviors associated with multifrequency excitation, secondary resonances, and second-order approximation.

The two works noted above give a good review of prior studies on parametrically excited moving media. Particularly relevant studies include the work of Mahalingam [3], Mote [4,5], Naguleswaran and Williams [6], and Asokanthan and Ariaratnam [7]. Recent studies include Oz et al. [8] and Chakraborty and Mallik [9]. Ulsoy et al. [10] motivated the studies for automotive belt drives by showing a primary source of transverse belt vibration to be parametric instability caused by tension fluctuation.

Problem Formulation

The system is a beam/string of length L moving with time-dependent transport velocity $c(T)$. The equation of motion for transverse vibration is

$$\rho A (V_{TT} + c_T V_x + 2c V_{TX} + c^2 V_{XX}) - (P_d + P_s) V_{XX} + EIV_{XXXX} = 0 \quad (1)$$

where ρA is the mass per unit length, EI is the bending stiffness, V is the transverse displacement, T is the time, X is the spatial coordinate, P_s is the mean belt tension, and $P_d(T)$ is the dynamic tension. The dynamic tension results from longitudinal belt motion and midplane stretching from transverse deflection. Under the assumption of quasi-static stretching ([11]), the dynamic tension is

$$P_d = \frac{EA}{L} \left[U(L, T) - U(0, T) + \frac{1}{2} \int_0^L V_x^2 dX \right] \quad (2)$$

where EA is the longitudinal stiffness modulus and U is the longitudinal displacement. Use of the dimensionless parameters

$$x, v, u = \frac{X, V, U}{L}, \quad t = \sqrt{\frac{P_s}{\rho A L^2}} T, \quad \gamma = c / \sqrt{\frac{P_s}{\rho A}}, \quad (3)$$

$$\zeta = \frac{EA}{P_s}, \quad \alpha = \frac{EI}{P_s L^2}$$

¹To whom correspondence should be addressed

Contributed by the Applied Mechanics Division of THE AMERICAN SOCIETY OF MECHANICAL ENGINEERS for publication in the ASME JOURNAL OF APPLIED MECHANICS. Manuscript received by the ASME Applied Mechanics Division, Aug. 26, 1999; final revision, June 27, 2000. Associate Editor: A. K. Mal. Discussion on the paper should be addressed to the Editor, Professor Lewis T. Wheeler, Department of Mechanical Engineering, University of Houston, Houston, TX 77204-4792, and will be accepted until four months after final publication of the paper itself in the ASME JOURNAL OF APPLIED MECHANICS.

gives

$$v_{tt} + 2\gamma v_{tx} + \gamma v_x - (1 - \gamma^2)v_{xx} + \alpha v_{xxx} - \zeta \left[u(1,t) - u(0,t) + \frac{1}{2} \int_0^1 v_x^2 dx \right] v_{xx} = 0. \quad (4)$$

The relative longitudinal motion of the end points, which results from rotational pulley oscillations, consists of multifrequency excitation of the form

$$\zeta [u(1,t) - u(0,t)] = \zeta \sum_{i=1}^k u_i \cos(\Omega_i t + \theta_i) = \sum_{i=1}^k \varepsilon_i \cos(\Omega_i t + \theta_i). \quad (5)$$

$\varepsilon_i = (EA u_i) / P_s < 1$ represents the ratio of the dynamic tension fluctuation caused by the i th spectral component of the relative endpoint motion to the mean span tension. The relative longitudinal motion of the endpoints $u(1,t) - u(0,t)$ is specified. In serpentine belt drives, it is calculated from dynamic analysis of the discrete pulley rotations induced by crankshaft excitations and dynamic accessory torques. Engine firing pulses cause a speed ‘ripple’ on the mean crankshaft rotation speed. The associated belt speed fluctuations are

$$\gamma = \gamma_0 + \sum_{i=1}^{k'} \varepsilon'_i \sin(\Omega'_i t + \theta'_i). \quad (6)$$

Typically, the dominant speed and tension fluctuation frequency equals $N/2$ times the engine speed, where N is the number of cylinders, though higher harmonics of this frequency and accessory torque frequencies are also present. The dimensionless frequencies are related to the dimensional ones (Ω_i^*) by $\Omega_i = \sqrt{\rho A L^2 / P_s} \Omega_i^*$. From (4), the linearized equation of motion with tension and speed fluctuations is

$$v_{tt} + 2\gamma_0 v_{tx} - (1 - \gamma_0^2)v_{xx} + \alpha v_{xxx} - \sum_{i=1}^k \varepsilon_i \cos(\Omega_i t + \theta_i) v_{xx} + \sum_{i=1}^{k'} \varepsilon'_i \{ 2v_{tx} \sin(\Omega'_i t + \theta'_i) + 2\gamma_0 v_{xx} \sin(\Omega'_i t + \theta'_i) + \Omega'_i v_x \cos(\Omega'_i t + \theta'_i) \} + \left(\sum_{i=1}^{k'} \varepsilon'_i \sin(\Omega'_i t + \theta'_i) \right)^2 v_{xx} = 0. \quad (7)$$

For subsequent discretization, it is convenient to rewrite (7) in state space form as

$$A W_t + B W + \sum_{i=1}^{k'} \varepsilon'_i \{ \sin(\Omega'_i t + \theta'_i) C + \Omega'_i \cos(\Omega'_i t + \theta'_i) D \} W - \sum_{i=1}^k \varepsilon_i \cos(\Omega_i t + \theta_i) E W + \left(\sum_{i=1}^{k'} \varepsilon'_i \sin(\Omega'_i t + \theta'_i) \right)^2 E W = 0 \quad (8)$$

$$A = \begin{bmatrix} 1 & 0 \\ 0 & -(1 - \gamma_0^2) \frac{\partial^2}{\partial x^2} + \alpha \frac{\partial^4}{\partial x^4} \end{bmatrix},$$

$$B = \begin{bmatrix} 2\gamma_0 \frac{\partial}{\partial x} & -(1 - \gamma_0^2) \frac{\partial^2}{\partial x^2} + \alpha \frac{\partial^4}{\partial x^4} \\ (1 - \gamma_0^2) \frac{\partial^2}{\partial x^2} - \alpha \frac{\partial^4}{\partial x^4} & 0 \end{bmatrix},$$

$$C = \begin{bmatrix} 2 \frac{\partial}{\partial x} & 2\gamma_0 \frac{\partial^2}{\partial x^2} \\ 0 & 0 \end{bmatrix}, \quad D = \begin{bmatrix} 0 & \frac{\partial}{\partial x} \\ 0 & 0 \end{bmatrix},$$

$$E = \begin{bmatrix} 0 & \frac{\partial^2}{\partial x^2} \\ 0 & 0 \end{bmatrix}, \quad W = \begin{bmatrix} v_t \\ v \end{bmatrix}. \quad (9)$$

The inner product in the state space is $\langle W, V \rangle = \int_0^1 W^T \bar{V} dx$, where the overbar denotes complex conjugate and superscript T denotes transpose.

The Galerkin basis consists of the state-space eigenfunctions for the nonparametrically excited system (8) ([12])

$$\Phi_n = \begin{bmatrix} j\omega_n \psi_n \\ \psi_n \end{bmatrix} = \begin{bmatrix} \lambda_n \psi_n \\ \psi_n \end{bmatrix} \quad (10)$$

where ψ_n are the complex eigenfunctions of (7) ($\varepsilon_i = \varepsilon'_i = 0$) and ω_n are the natural frequencies. The Φ_n possess the orthonormality properties $\langle A \Phi_n, \Phi_m \rangle = \delta_{mn}$, $\langle B \Phi_n, \Phi_m \rangle = -\lambda_n \delta_{mn} = -j\omega_n \delta_{mn}$. For the moving string model ($\alpha = 0$) the eigensolutions are

$$\psi_n = \frac{1}{n\pi\sqrt{1 - \gamma_0^2}} e^{jn\pi\gamma_0 x} \sin(n\pi x), \quad \lambda_n = j\omega_n = jn\pi(1 - \gamma_0^2) \quad (11)$$

for fixed pulleys at the string supports. Eigensolutions for a traveling beam can not be expressed in closed form and require numerical solution ([4]).

Multifrequency Parametric Instabilities

To investigate primary parametric instabilities, we use a single-term Galerkin discretization for the n th mode obtained by use of one traveling system basis function

$$W = \xi_n(t) \Phi_n(x) + \bar{\xi}_n(t) \bar{\Phi}_n(x) = 2 \operatorname{Re}[\xi_n(t) \Phi_n(x)]. \quad (12)$$

Mockensturm et al. [1] demonstrated the excellent convergence achieved with this single term expansion for a string model. Substituting (12) into (8) and taking the inner product with Φ_n yields the complex, time-varying equation (the notation $E_{nm} = \langle E \Phi_n, \Phi_m \rangle$, $E_{\bar{n}m} = \langle E \bar{\Phi}_n, \Phi_m \rangle$, $\bar{E}_{nm} = \overline{\langle E \Phi_n, \Phi_m \rangle}$, etc., and similar relations for the C and D operators are used throughout)

$$\dot{\xi}_n - j\omega_n \xi_n - \left[\varepsilon \sum_{i=1}^k f_i \cos(\Omega_i t + \theta_i) \right] (\xi_n E_{nn} + \bar{\xi}_n E_{\bar{n}n}) + \left[\varepsilon \sum_{i=1}^{k'} f'_i \sin(\Omega'_i t + \theta'_i) \right] (\xi_n C_{nn} + \bar{\xi}_n C_{\bar{n}n}) + \left[\varepsilon \sum_{i=1}^{k'} f'_i \Omega'_i \cos(\Omega'_i t + \theta'_i) \right] (\xi_n D_{nn} + \bar{\xi}_n D_{\bar{n}n}) = 0, \quad n = 1, 2, \dots \quad (13)$$

where all the excitations are taken to be of the same order, that is

$$\varepsilon_i = \varepsilon f_i, \quad \varepsilon'_i = \varepsilon f'_i, \quad f_i, f'_i = 0(1). \quad (14)$$

Based on the Floquet theory ([13]), combinations of parametric excitation frequency and amplitude for which (13) has periodic solutions separate the regions of bounded and unbounded motions. These stability boundaries are sought in the form of perturbation expansions ([11]),

$$\xi_n = p_0 + \varepsilon p_1 + \varepsilon^2 p_2, \quad \omega_n = \bar{\omega}_n + \varepsilon r_1 + \varepsilon^2 r_2. \quad (15)$$

For simplicity, the body of the paper examines the case of tension excitation alone ($\varepsilon'_i = 0$), where (13) reduces to

$$\begin{aligned} \dot{\xi}_n - j\omega_n \xi_n - \left[\varepsilon \sum_{i=1}^k f_i \cos(\Omega_i t + \theta_i) \right] (\xi_n E_{nn} + \bar{\xi}_n E_{\bar{n}n}) = 0 \\ n = 1, 2, \dots \end{aligned} \quad (16)$$

Stability results for speed fluctuations and simultaneous tension and speed fluctuations are given in the Appendix. Substitution of (15) into (16) gives the sequence of perturbation problems

$$\begin{aligned} \dot{p}_0 - j\bar{\omega}_n p_0 = 0 \\ \dot{p}_1 - j\bar{\omega}_n p_1 = jr_1 p_0 + \left[\sum_{i=1}^k f_i \cos(\Omega_i t + \theta_i) \right] [p_0 E_{nn} + \bar{p}_0 E_{\bar{n}n}] \end{aligned} \quad (17)$$

$$\begin{aligned} \dot{p}_2 - j\bar{\omega}_n p_2 = jr_1 p_1 + jr_2 p_0 \\ + \left[\sum_{i=1}^k f_i \cos(\Omega_i t + \theta_i) \right] [p_1 E_{nn} + \bar{p}_1 E_{\bar{n}n}]. \end{aligned} \quad (18)$$

The periodic solution of (17) is

$$p_0 = a e^{i\bar{\omega}_n t}. \quad (20)$$

Substitution of (20) into (18) yields

$$\begin{aligned} \dot{p}_1 - j\bar{\omega}_n p_1 = jr_1 a e^{j\bar{\omega}_n t} + \sum_{i=1}^k \frac{f_i}{2} \{ a E_{nn} [e^{j[(\Omega_i + \bar{\omega}_n)t + \theta_i]} \\ + e^{-j[(\Omega_i - \bar{\omega}_n)t + \theta_i]}] \\ + \bar{a} E_{\bar{n}n} [e^{j[(\Omega_i - \bar{\omega}_n)t + \theta_i]} + e^{-j[(\Omega_i + \bar{\omega}_n)t + \theta_i]}] \}. \end{aligned} \quad (21)$$

1 Primary Instability. In general, the sole secular term in (21) is $jr_1 a e^{j\bar{\omega}_n t}$ and its elimination leads to the trivial solution ($a=0$) or $r_1=0$ (secondary instability, considered later). When any excitation frequency is near $2\omega_n$, however, additional secular terms exist. In this case, $\Omega_i \approx 2\omega_n$ (that is, $\Omega_i = 2\bar{\omega}_n$) and $\Omega_i \neq 2\omega_n$ for $i \neq l$. The periodicity condition demands that secular terms vanish, yielding

$$jr_1 a + \frac{f_l}{2} \bar{a} E_{\bar{n}n} e^{j\theta_l} = 0. \quad (22)$$

Separating the real and imaginary parts leads to

$$\begin{bmatrix} -r_1 + \frac{f_l}{2} \text{Im}(E_{\bar{n}n} e^{j\theta_l}) & \frac{f_l}{2} \text{Re}(E_{\bar{n}n} e^{j\theta_l}) \\ -\frac{f_l}{2} \text{Re}(E_{\bar{n}n} e^{j\theta_l}) & r_1 + \frac{f_l}{2} \text{Im}(E_{\bar{n}n} e^{j\theta_l}) \end{bmatrix} \begin{bmatrix} \text{Im}(a) \\ \text{Re}(a) \end{bmatrix} = 0. \quad (23)$$

For a nontrivial solution of (23) to exist,

$$r_1 = \pm \frac{f_l}{2} |E_{\bar{n}n}|. \quad (24)$$

With $r_1 = \pm (f_l/2)|E_{\bar{n}n}|$, a solution of (21) is

$$\begin{aligned} p_1 = b e^{j\bar{\omega}_n t} + \sum_{i=1}^k j \frac{f_i a E_{nn}}{2\Omega_i} [-e^{j[(\Omega_i + \bar{\omega}_n)t + \theta_i]} + e^{-j[(\Omega_i - \bar{\omega}_n)t + \theta_i]}] \\ - \sum_{i=1, i \neq l}^k j \frac{f_i \bar{a} E_{\bar{n}n}}{2(\Omega_i - \Omega_l)} e^{j[(\Omega_i - \bar{\omega}_n)t + \theta_i]} \\ + \sum_{i=1}^k j \frac{f_i \bar{a} E_{\bar{n}n}}{2(\Omega_i + \Omega_l)} e^{-j[(\Omega_i + \bar{\omega}_n)t + \theta_i]}. \end{aligned} \quad (25)$$

Substitution of (20) and (25) into (19) yields

$$\begin{aligned} \dot{p}_2 - j\bar{\omega}_n p_2 = jr_2 a e^{j\bar{\omega}_n t} + jr_1 b e^{j\bar{\omega}_n t} + \frac{f_l}{2} E_{\bar{n}n} \bar{b} e^{j(\bar{\omega}_n t + \theta_l)} \\ + j \sum_{i=1, i \neq l}^k \frac{f_i^2 a |E_{\bar{n}n}|^2}{4(\Omega_i - \Omega_l)} e^{j\bar{\omega}_n t} - j \sum_{i=1}^k \frac{f_i^2 a |E_{\bar{n}n}|^2}{4(\Omega_i + \Omega_l)} e^{j\bar{\omega}_n t} \\ + \text{N.S.T.} \end{aligned} \quad (26)$$

where N.S.T. denotes nonsecular terms. Elimination of secular terms from p_2 requires

$$\begin{aligned} jr_1 b + \frac{f_l}{2} \bar{b} E_{\bar{n}n} e^{j\theta_l} = -ja \left\{ r_2 + |E_{\bar{n}n}|^2 \left[\sum_{i=1, i \neq l}^k \frac{f_i^2}{4(\Omega_i - \Omega_l)} \right. \right. \\ \left. \left. - \sum_{i=1}^k \frac{f_i^2}{4(\Omega_i + \Omega_l)} \right] \right\}. \end{aligned} \quad (27)$$

Considering $\text{Re}(b)$ and $\text{Im}(b)$ as the unknowns, (22)–(24) show that the coefficient matrix in (27) is singular. The solvability condition for (27) leads to r_2 , and the final boundary curves are obtained from (15) as

$$\begin{aligned} \omega_n = \frac{\Omega_l}{2} \pm \frac{\varepsilon_l}{2} |E_{\bar{n}n}| + |E_{\bar{n}n}|^2 \left[- \sum_{i=1, i \neq l}^k \frac{\varepsilon_i^2}{4(\Omega_i - \Omega_l)} \right. \\ \left. + \sum_{i=1}^k \frac{\varepsilon_i^2}{4(\Omega_i + \Omega_l)} \right]. \end{aligned} \quad (28)$$

Using $\Omega_l = 2\omega_n + O(\varepsilon)$, (28) is converted to

$$\Omega_l = 2\omega_n \pm \varepsilon_l |E_{\bar{n}n}| - |E_{\bar{n}n}|^2 \left[- \sum_{i=1, i \neq l}^k \varepsilon_i^2 \frac{2\omega_n}{\Omega_i^2 - 4\omega_n^2} + \frac{\varepsilon_l^2}{8\omega_n} \right]. \quad (29)$$

Equation (29) applies for moving, tensioned beams. When specialized to the moving string ($\alpha=0$), the result (29) can be expressed entirely in terms of system parameters with the following expressions obtained from (11):

$$E_{\bar{n}n} = (1 - e^{-2jn\pi\gamma_0}) / (4\gamma_0), \quad E_{nn} = jn\pi(1 + \gamma_0^2) / 2. \quad (30)$$

Up to the first order of perturbation, the stability boundaries as given by (29) are determined solely by the root cause parametric excitation $\Omega_l \approx 2\omega_n$ with no effect from excitations at other frequencies (see Eq. (24)). Changes in the stability boundaries caused by the presence of multiple parametric excitation terms are evident at higher orders of perturbation. Note that the primary instability boundaries (29) are not affected by the phase angles θ_i between the multiple excitations. These features are also reflected in the stability boundaries for speed excitation and simultaneous speed and tension excitation derived from (13) ((52) and (55) in the Appendix). In the simultaneous tension and speed excitation case ((55)–(57)), the tension and speed fluctuations share a common frequency component that excites instability. This is typical of automotive belt drives where the tension and speed both fluctuate at the engine firing frequency.

Figure 1 compares the stability boundaries for a moving string ($\alpha=0$) under two simultaneous tension excitations ($\varepsilon_i^2=0$) obtained by three methods: first-order perturbation, second-order perturbation, and numerical methods. $\Omega_1 \approx 2\omega_1$ is the root cause of primary instability. Numerical boundaries are determined by examining the eigenvalues of the numerically integrated fundamental matrix of (16) for varying Ω_1 and ε_1 . The first-order stability boundaries (dotted lines) do not capture the effects of the second parametric excitation (Ω_2) and are the same as for mono-frequency excitation. The second-order boundaries reflect the impact of the second excitation, and the entire instability region shifts (solid lines). The classical result that parametric instability

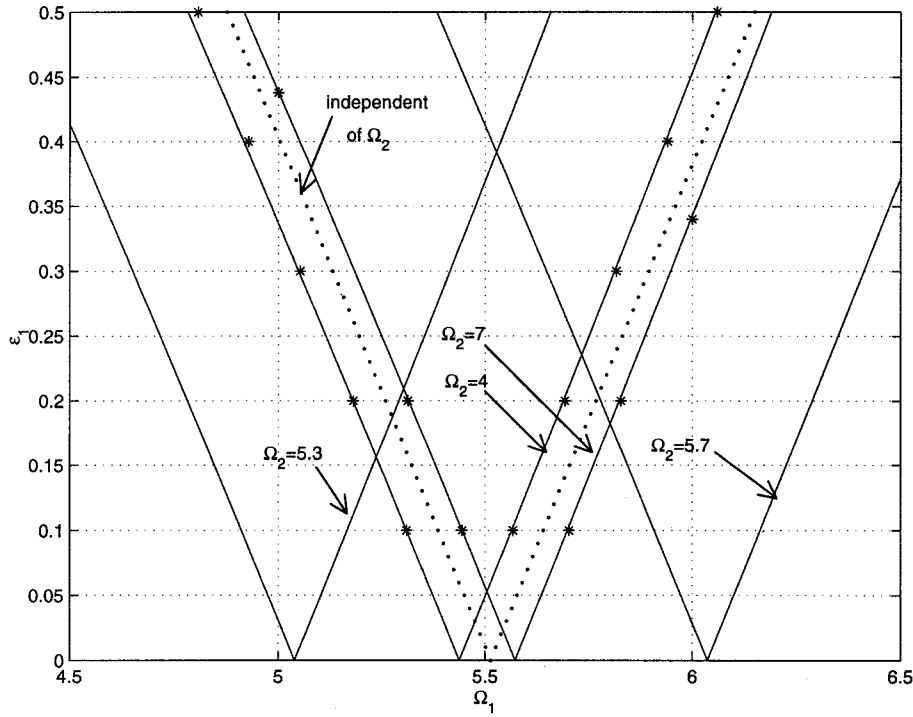


Fig. 1 Comparison among numerical results (*), first-order perturbation (dots) and second-order perturbation (solid curves) of the first mode ($\omega_1=2.76$) primary instability region of an axially moving string under two parametric tension excitations. $\gamma=0.35$, $\varepsilon_2=0.35$.

occurs when an excitation frequency is twice a natural frequency does not hold when multiple parametric excitations are present. To see this, consider (29) when two excitations exist,

$$\Omega_1 = 2\omega_n \pm \varepsilon_1 |E_{\bar{n}n}| - |E_{\bar{n}n}|^2 \left[\frac{\varepsilon_1^2}{8\omega_n} - \frac{2\varepsilon_2^2\omega_n}{(\Omega_2^2 - 4\omega_n^2)} \right].$$

Because of the excitation at frequency Ω_2 , the cusp ($\varepsilon_1 \rightarrow 0$) moves from $\Omega_1 = 2\omega_n$ to $\Omega_1 = 2\omega_n + 2|E_{\bar{n}n}|^2\varepsilon_2^2\omega_n / (\Omega_2^2 - 4\omega_n^2)$. The whole instability region shifts accordingly, and parametric instability occurs at higher excitation frequency ($\Omega_1 > 2\omega_n$) when $\Omega_2 > 2\omega_n$ and lower excitation frequency ($\Omega_1 < 2\omega_n$) when $\Omega_2 < 2\omega_n$. Note that a separate analysis including additional secular terms is required for the case $\Omega_2 \approx \Omega_1 \approx 2\omega_n$.

The continuous dependence of the first mode primary instability region with the two excitation amplitudes $\varepsilon_{1,2}$ is illustrated in Fig. 2. Ω_1 causes the primary instability. The shift of the instability region away from $\Omega_1 = 2\omega_1$ due to the second excitation is apparent from the drift in the cusp at $\varepsilon_1 = 0$.

2 Secondary Instability. Primary instabilities are characterized by a response frequency of half the parametric excitation frequency. In automotive belt drives, however, transverse belt vibration frequently occurs where the belt frequency is the same as the engine firing frequency. This is characteristic of secondary instability where a parametric excitation frequency is close to one of the system natural frequencies ($\Omega_i \approx \omega_n$).

In the absence of primary instability, the only secular term in (21) is $jr_1 a e^{j\bar{\omega}_n t}$. Specifying $r_1 = 0$, (25) is again a solution of (21) except the second summation allows any value of i . Substitution of this solution into (19) yields

$$\begin{aligned} \dot{p}_2 - j\bar{\omega}_n p_2 = & jr_2 a e^{j\bar{\omega}_n t} \\ & - j \sum_{i=1}^k \sum_{p=1}^k \frac{f_i f_p \bar{a} E_{\bar{n}n} E_{nn}}{4(\Omega_p - 2\bar{\omega}_n)} e^{j[(\Omega_i + \Omega_p - \bar{\omega}_n)t + (\theta_i + \theta_p)]} \\ & - j \sum_{i=1}^k \sum_{p=1}^k \frac{f_i f_p \bar{a} E_{\bar{n}n} \bar{E}_{nn}}{4\Omega_p} e^{j[(\Omega_i + \Omega_p - \bar{\omega}_n)t + (\theta_i + \theta_p)]} \\ & + j \sum_{i=1}^k \frac{f_i^2 a |E_{\bar{n}n}|^2}{4(\Omega_i - 2\bar{\omega}_n)} e^{j\bar{\omega}_n t} - j \sum_{i=1}^k \frac{f_i^2 a |E_{\bar{n}n}|^2}{4(\Omega_i + 2\bar{\omega}_n)} e^{j\bar{\omega}_n t} \\ & + \text{N.S.T.} \end{aligned} \quad (31)$$

Elimination of secular terms in (31) for the case when $\Omega_i \approx \omega_n$ and $\Omega_l \neq \omega_n$ for $i \neq l$ leads to the secondary instability boundaries

$$\begin{aligned} \Omega_l = \omega_n \pm \frac{\varepsilon_l^2}{\omega_n} \text{Im}(E_{nn}) |E_{\bar{n}n}| \\ - |E_{\bar{n}n}|^2 \left[- \sum_{i=1, i \neq l}^k \varepsilon_i^2 \frac{\omega_n}{\Omega_i^2 - 4\omega_n^2} + \frac{\varepsilon_l^2}{3\omega_n} \right]. \end{aligned} \quad (32)$$

Analogous results for speed and tension/speed excitation are given in the Appendix.

3 Simultaneous Primary and Secondary Instability. In a system under multiple parametric excitations, a mode may be simultaneously excited to primary instability by one excitation and secondary instability by another. This situation is expected in automotive belt drives as discussed later. With simultaneous instability, the instability boundaries may be significantly different from those of either excitation acting individually. Figure 3(a) shows the first mode primary and secondary instability boundaries for a moving string for a single excitation (Ω_1). The secondary

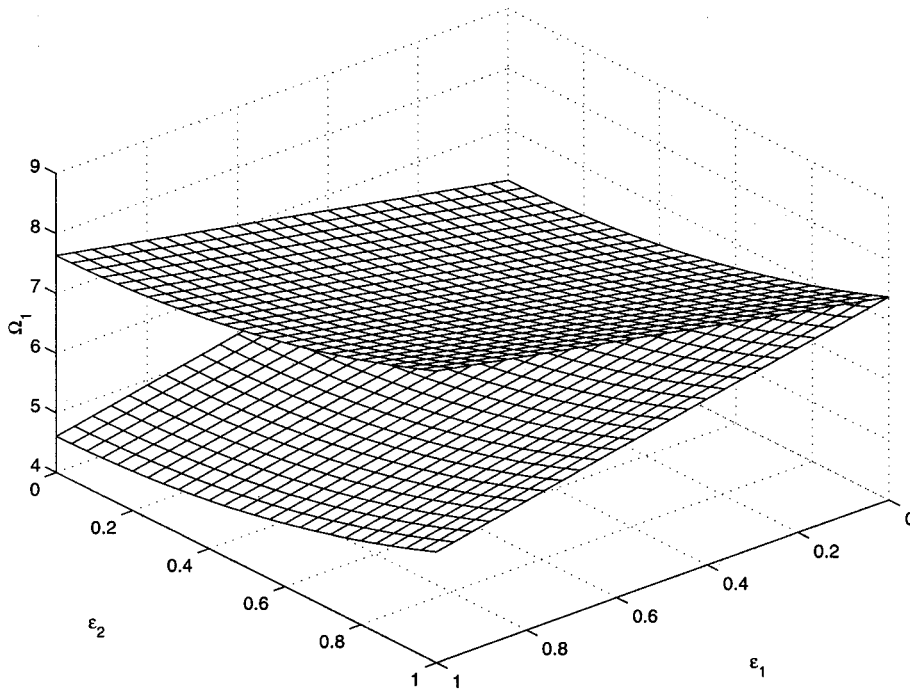


Fig. 2 Continuous dependence on excitation amplitudes of the first mode ($\omega_1=3.07$) primary instability region of an axially moving string under two parametric tension excitations. $\Omega_2=7, \gamma=0.15$.

instability region is characteristically much narrower than the primary one. When a second tension excitation exists with frequency $\Omega_2=2\Omega_1 \approx 2\omega_n$, primary instability from Ω_2 occurs near the secondary instability from Ω_1 . Perturbation analysis of this dual excitation case gives the instability region

$$\Omega_1 = \omega_n \pm \frac{\epsilon_2}{2} |E_{nn}| - |E_{nn}|^2 \left[\frac{\epsilon_1^2}{3\omega_n} + \frac{\epsilon_2^2}{16\omega_n} \right] \mp \frac{\epsilon_1^2}{\omega_n} \text{Im}(E_{nn}) |E_{nn}|. \quad (33)$$

As shown in Fig. 3(b), the coincidence of the primary instability caused by Ω_2 and the secondary instability of Ω_1 significantly widens the secondary instability region. Notice that the unstable region is *wider* for small ϵ_1 . Considering the dual excitation case with $\Omega_2=(1/2)\Omega_1$, the presence of a simultaneous secondary instability from Ω_2 impacts the primary instability at $\Omega_1 \approx 2\omega_n$ as seen by comparing Figs. 3(a) and 3(c). Here, the primary instability region narrows overall and *closes* for nonzero amplitude of the excitation causing primary instability ($\epsilon_1 \approx 0.1$). This phenomenon is further depicted in Figs. 4 and 5 for instability in the second mode. Figures 4(a) and 4(b) contrast the dependence of the second mode primary instability region on excitation amplitude and speed for the cases with and without simultaneous secondary instability. In Fig. 4(b), notice that the instability region closes for nonzero $\epsilon_1 \approx 0.3$ even though each of the Ω_1 and Ω_2 excitations induce instability individually. While the width of the primary instability regions widen with excitation amplitude (Fig. 4(a)), the width of the simultaneous primary/secondary region may decrease with excitation amplitude (Fig. 4(b) for small ϵ_1). One can see similar interplay between the primary and secondary instabilities in Fig. 5, which is analogous to Fig. 4 except the focus is on the secondary instability.

The widening of the secondary instability region ($\Omega_1 \approx \omega_n$) when a second excitation $\Omega_2=2\Omega_1 \approx 2\omega_n$ is present (Fig. 3(b)) has implications for practical systems. In automotive belt drives (and other systems), the excitation is periodic but not sinusoidal. Because of the integer harmonics of the fundamental frequency (the firing frequency in automotive belt drives) in the excitation

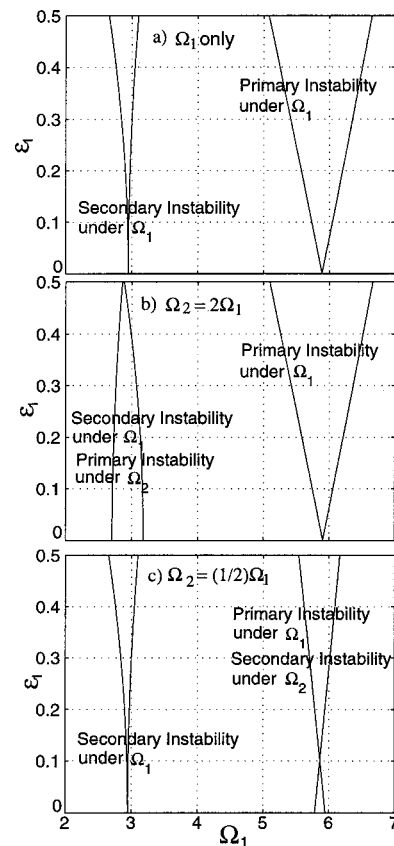


Fig. 3 First mode ($\omega_1=2.95$) stability boundaries of an axially moving string caused by three parametric excitation combinations for $\gamma=0.25$: (a) single excitation Ω_1 , (b) two excitations $\Omega_2=2\Omega_1, \epsilon_2=0.3$, and (c) two excitations $\Omega_2=(1/2)\Omega_1, \epsilon_2=0.3$

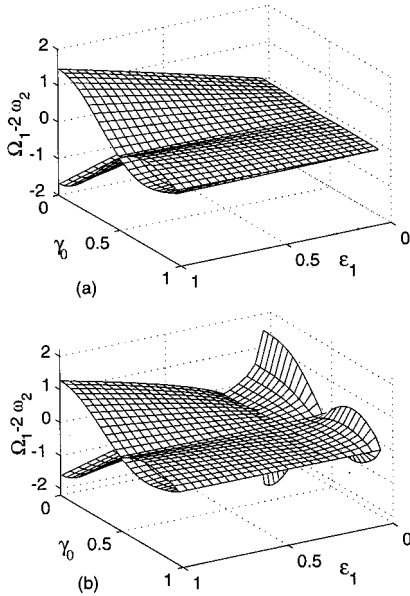


Fig. 4 Dependence of the second mode ($\omega_2=2\pi(1-\gamma_0^2)$) moving string principal instability region on translation speed for (a) single excitation, $\Omega_1 \approx 2\omega_2$, (b) two excitations, $\Omega_1 \approx 2\omega_2$ and $\Omega_2 = (1/2)\Omega_1 \approx \omega_2, \epsilon_2 = 0.3$

spectrum, simultaneous primary and secondary parametric instability is likely. This may explain the common observation of belt span vibration at the engine firing frequency in automotive drives. To explain these observations with a monofrequency excitation model of secondary instability, large excitation amplitudes are required because of the narrowness of the secondary instability region (Fig. 3(a)) and the inherent damping. The behavior is more plausibly understood with a multifrequency excitation model for realistic excitation amplitudes.

As the translation speed increases, both of the secondary and primary instability regions narrow and even close at some speeds

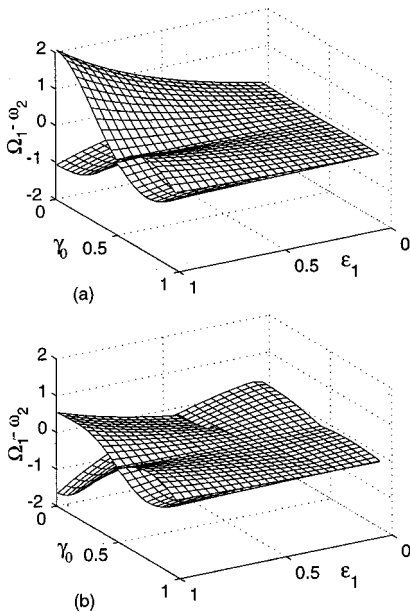


Fig. 5 Dependence of the second mode ($\omega_2=2\pi(1-\gamma_0^2)$) moving string secondary instability region on translation speed for (a) single excitation, $\Omega_1 \approx \omega_2$, (b) two excitations, $\Omega_1 \approx \omega_2$ and $\Omega_2 = 2\Omega_1 \approx 2\omega_2, \epsilon_2 = 0.3$

(Figs. 4(a) and 5(a)). As pointed out by Mockensturm et al. [1] for primary instability, there are n subcritical translation speeds where the n th mode primary instability region closes. The same holds true for secondary instability.

4 Combination Instability. This section addresses sum and difference type combination instabilities involving two modes. Taking the n th and m th modes, the discretized equations are obtained from the expansion

$$W = \xi_n(t)\Phi_n(x) + \bar{\xi}_n(t)\bar{\Phi}_n(x) + \xi_m(t)\Phi_m(x) + \bar{\xi}_m(t)\bar{\Phi}_m(x) = 2 \operatorname{Re}[\xi_n(t)\Phi_n(x) + \xi_m(t)\Phi_m(x)]. \quad (34)$$

Considering tension fluctuations only, use of (34) in Galerkin discretization of (8) yields

$$\begin{aligned} \dot{\xi}_n - j\omega_n \xi_n - \left[\varepsilon \sum_{i=1}^k f_i \cos(\Omega_i t + \theta_i) \right] \\ \times (\xi_n E_{nn} + \bar{\xi}_n E_{\bar{n}\bar{n}} + \xi_m E_{mn} + \bar{\xi}_m E_{\bar{m}\bar{m}}) \end{aligned} \quad (35)$$

$$\begin{aligned} \dot{\xi}_m - j\omega_m \xi_m - \left[\varepsilon \sum_{i=1}^k f_i \cos(\Omega_i t + \theta_i) \right] \\ \times (\xi_n E_{nm} + \bar{\xi}_n E_{\bar{n}\bar{m}} + \xi_m E_{mm} + \bar{\xi}_m E_{\bar{m}\bar{m}}). \end{aligned} \quad (36)$$

Motivated by the expected sum-type instability when $\Omega_i \approx \omega_n + \omega_m$, the solution forms are chosen as

$$\begin{aligned} \Omega_l &= (\omega_n + \omega_m) - 2\varepsilon r_1 - 2\varepsilon^2 r_2 \\ &= (\omega_n - \varepsilon r_1 - \varepsilon^2 r_2) + (\omega_m - \varepsilon r_1 - \varepsilon^2 r_2) = \bar{\omega}_n + \bar{\omega}_m \\ \Rightarrow \xi_n &= p_0 + \varepsilon p_1 + \varepsilon^2 p_2, \quad \xi_m = q_0 + \varepsilon q_1 + \varepsilon^2 q_2 \\ \omega_n &= \bar{\omega}_n + \varepsilon r_1 + \varepsilon^2 r_2, \quad \omega_m = \bar{\omega}_m + \varepsilon r_1 + \varepsilon^2 r_2. \end{aligned} \quad (37)$$

Substitution of (37) into (35) and (36) yields

$$\dot{p}_0 - j\bar{\omega}_n p_0 = 0, \quad \dot{q}_0 - j\bar{\omega}_m q_0 = 0 \quad (38)$$

$$\begin{aligned} \dot{p}_1 - j\bar{\omega}_n p_1 = j r_1 p_0 + \left[\sum_{i=1}^k f_i \cos(\Omega_i t + \theta_i) \right] [p_0 E_{nn} + \bar{p}_0 E_{\bar{n}\bar{n}} \\ + q_0 E_{mn} + \bar{q}_0 E_{\bar{m}\bar{m}}] \end{aligned} \quad (39)$$

$$\begin{aligned} \dot{q}_1 - j\bar{\omega}_m q_1 = j r_1 q_0 + \left[\sum_{i=1}^k f_i \cos(\Omega_i t + \theta_i) \right] [p_0 E_{nm} + \bar{p}_0 E_{\bar{n}\bar{m}} \\ + q_0 E_{mm} + \bar{q}_0 E_{\bar{m}\bar{m}}] \end{aligned} \quad (40)$$

and similar equations for p_2 and q_2 . The periodic solutions of (38) are $p_0 = a_n e^{j\bar{\omega}_n t}$, $q_0 = a_m e^{j\bar{\omega}_m t}$. With these solutions, elimination of secular terms in (39) and (40) for $\Omega_l \approx \omega_n + \omega_m$ requires

$$j r_1 a_n + \frac{f_1}{2} \bar{a}_m E_{\bar{m}\bar{n}} e^{j\theta_1} = 0, \quad j r_1 a_m + \frac{f_1}{2} \bar{a}_n E_{\bar{n}\bar{m}} e^{j\theta_1} = 0. \quad (41)$$

After solution of (41) and use of $\Omega_l = \omega_n + \omega_m + O(\varepsilon)$, (37) gives

$$\Omega_l = \omega_n \pm \omega_m + \varepsilon_l \sqrt{E_{\bar{n}\bar{m}} \bar{E}_{\bar{m}\bar{n}}} \quad (42)$$

A natural extension to second-order perturbation was also calculated. As with primary and secondary instabilities, these boundaries are independent of the phasing between the different excitation frequencies. Figure 6 shows the sum type instability region of a moving string under tension fluctuation obtained by first and second-order perturbation. Note the scaling of Fig. 6; the combination instability region is much narrower than the primary instability region (Fig. 1). The effects from multiple excitation frequencies, including the shift of the entire instability region, are minimal, and first-order approximations that do not capture these

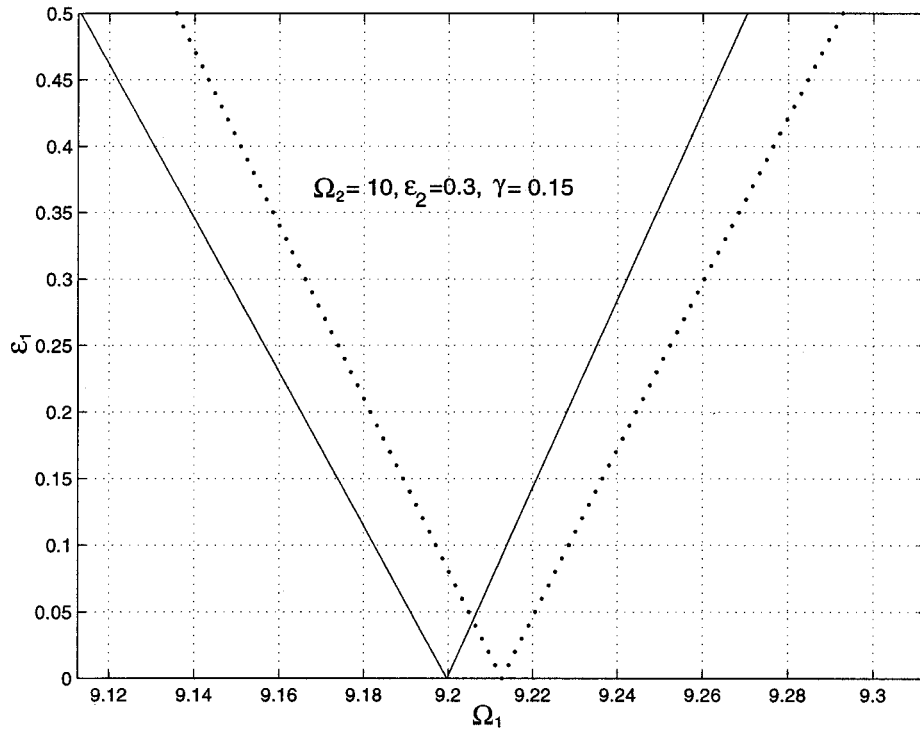


Fig. 6 Moving string stability boundaries of first ($\omega_1=3.071$) and second mode ($\omega_2=6.142$) sum-type combination instability ($\Omega_1 \approx \omega_1 + \omega_2$) for two parametric tension excitations. Dotted curves denote first-order perturbation, and solid curves denote second-order perturbation.

effects appear justified for practical systems. See the Appendix for speed excitation and simultaneous speed and tension excitation results.

To examine possible difference type combination instabilities where $\Omega_l \approx \omega_n - \omega_m$, the approximate solutions are constructed as

$$\begin{aligned} \Omega_l &= (\omega_n - \omega_m) - 2\varepsilon r_1 - 2\varepsilon^2 r_2 \\ &= (\omega_n - \varepsilon r_1 - \varepsilon^2 r_2) - (\omega_m + \varepsilon r_1 + \varepsilon^2 r_2) = \tilde{\omega}_n + \tilde{\omega}_m \\ \Rightarrow \xi_n &= p_0 + \varepsilon p_1 + \varepsilon^2 p_2, \quad \xi_m = q_0 + \varepsilon q_1 + \varepsilon^2 q_2 \\ \Rightarrow \omega_n &= \tilde{\omega}_n + \varepsilon r_1 + \varepsilon^2 r_2, \quad \omega_m = \tilde{\omega}_m - \varepsilon r_1 - \varepsilon^2 r_2 \end{aligned} \quad (43)$$

In this case, the first-order stability boundaries are

$$\Omega_l = (\omega_n - \omega_m) \pm \varepsilon_l \sqrt{E_{mn} E_{nm}} \quad (44)$$

Closed-form evaluation of the inner products in (44) gives complex values for Ω_l . This implies that there are no difference type instabilities up to first-order perturbation.

The results given in (29), (32), (33), (42), and the Appendix generalize those of Mockensturm et al. [1], where tension fluctuation is examined, and Pakdemirli and Ulsoy [2], where speed fluctuation is considered. In those analyses, the parametric excitation is restricted to a single harmonic term of either tension or speed excitation, only first-order approximations are derived, and secondary instabilities are not investigated.

Nonlinear Response Amplitude for Primary Instability

By including the midplane stretching nonlinearity in (4), transverse vibration amplitudes are determined for the principal parametric resonance regions. Allowing moderate displacements with the ordering $v = O(\sqrt{\varepsilon})$ ([1]), the nonlinear form of (7) is

$$\begin{aligned} A W_t + B W + \varepsilon \sum_{i=1}^{k'} f_i' \cos(\Omega_i' t + \theta_i') \{ \sin(\Omega_i' t + \theta_i') C \\ + \Omega_i' \cos(\Omega_i' t + \theta_i') D \} W \\ - \varepsilon \left(\sum_{i=1}^k f_i \cos(\Omega_i t + \theta_i) + \frac{1}{2} \zeta \int_0^1 v_x^2 dx \right) E W \\ + \left(\varepsilon \sum_{i=1}^{k'} f_i' \sin(\Omega_i' t + \theta_i') \right)^2 E W = 0. \end{aligned} \quad (45)$$

Galerkin discretization of (45) using (12) yields

$$\begin{aligned} \xi_n - j \omega_n \xi_n - \varepsilon \left[\sum_{i=1}^k f_i \cos(\Omega_i t + \theta_i) + \frac{1}{2} (d_1 \xi_n^2 + d_2 \xi_n \bar{\xi}_n + d_3 \bar{\xi}_n^2) \right] \\ \times (\xi_n E_{nn} + \bar{\xi}_n E_{\bar{n}\bar{n}}) + \varepsilon \sum_{i=1}^{k'} f_i' \{ \sin(\Omega_i' t + \theta_i') (\xi_n C_{nn} + \bar{\xi}_n C_{\bar{n}\bar{n}}) \\ + \Omega_i' \cos(\Omega_i' t + \theta_i') (\xi_n D_{nn} + \bar{\xi}_n D_{\bar{n}\bar{n}}) \} \\ + \left(\varepsilon \sum_{i=1}^{k'} \sin(\Omega_i' t + \theta_i') \right)^2 (\xi_n \langle E \Phi_n, \Phi_n \rangle + \bar{\xi}_n \langle E \bar{\Phi}_n, \bar{\Phi}_n \rangle) \\ = 0 \quad n=1, 2, \dots \end{aligned} \quad (46)$$

$$\begin{aligned} d_1 &= \int_0^1 \left(\frac{d\psi_n}{dx} \right)^2 dx, \quad d_2 = \int_0^1 \left(\frac{d\psi_n}{dx} \frac{d\bar{\psi}_n}{dx} \right) dx, \\ d_3 &= \int_0^1 \left(\frac{d\bar{\psi}_n}{dx} \right)^2 dx. \end{aligned} \quad (47)$$

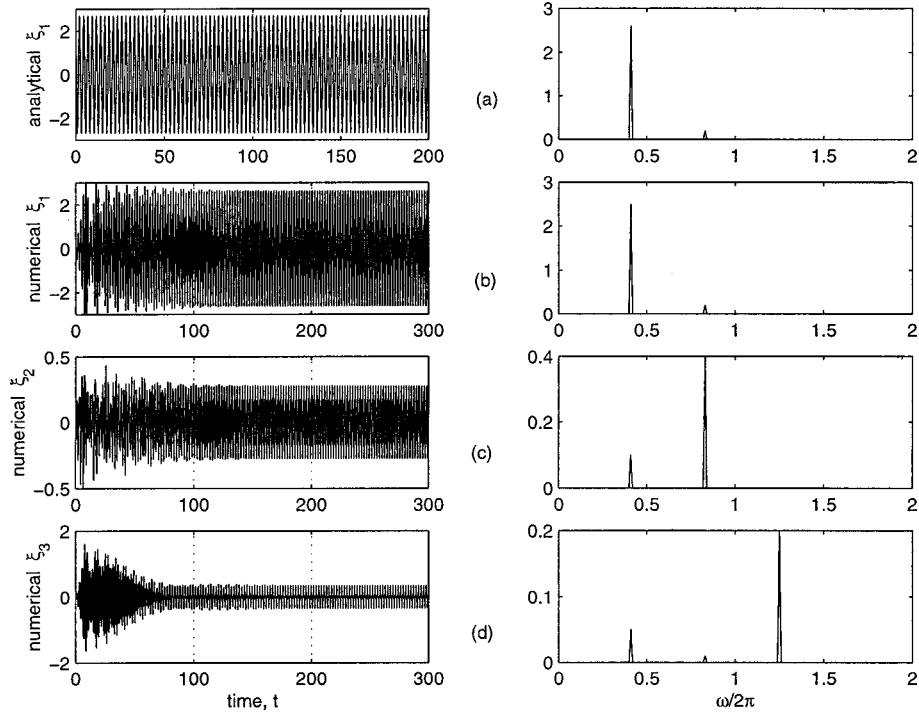


Fig. 7 Time histories and spectra of the modal response under first-mode primary instability with single frequency tension excitation. (a) analytical approximation, (b)–(d) numerical integration of coupled equations from a three-mode Galerkin discretization. $\gamma = 0.4$, $\omega_1 = 0.84\pi$, $\varepsilon_1 = 0.35$, $\sigma = -0.2$, $\Omega_1 = 2\omega_1 - 2\varepsilon_1\sigma = 1.68\pi$.

The method of multiple scales is applied to (46) with the expansion

$$\xi_n(t; \varepsilon) = p_0(t, \tau) + \varepsilon p_1(t, \tau) \quad (48)$$

where t and $\tau = \varepsilon t$ are the fast and slow time scales. The time derivative is defined as $d/dt \rightarrow \partial/\partial t + \varepsilon(\partial/\partial \tau)$. Insertion of (48) into (46) gives $\partial p_0/\partial t - j\omega_n p_0 = 0$ and a similar inhomogeneous equation for p_1 .

The problem of interest is that when speed and tension fluctuation share a common frequency component that simultaneously causes primary instability, that is $\Omega_l = \Omega'_l \approx 2\omega_n$. The nearness of Ω_l and Ω'_l to $2\omega_n$ is represented by $\Omega_l = \Omega'_l = 2\omega_n - 2\varepsilon\sigma$, where $\sigma = O(1)$. With the solution $p_0 = K_n(\tau)e^{j\omega_n t} = \rho_n(\tau)e^{j(\beta_n(\tau) + \sigma\tau)}e^{j\omega_n t}$, elimination of secular terms in the differential equation for p_1 yields the conditions

$$\begin{aligned} \frac{d\rho_n}{d\tau} &= \varepsilon \rho_n [Q_n \sin(2\beta_n) + P_n \cos(2\beta_n) + R_n \rho_n^2] \\ \frac{d\beta_n}{d\tau} &= \varepsilon \left[-\frac{\sigma}{2} - P_n \sin(2\beta_n) + Q_n \cos(2\beta_n) + S_n \rho_n^2 \right] \end{aligned} \quad (49)$$

where P_n, Q_n , respectively, are the real and imaginary parts of $[-(f'_1/2)(jC_{nn} + \Omega'_l D_{nn}) + (f_1/2)E_{nn}]$ and R_n, S_n are the real and imaginary parts of $(\zeta/2)[d_2 E_{nn} + d_1 E_{nn}]$. The nontrivial equilibria of (49) are

$$(\rho_n^0)^2 = \frac{\sigma S_n \pm \sqrt{(\sigma S_n)^2 - 4(R_n^2 + S_n^2) \left(\frac{\sigma^2}{4} - P_n^2 - Q_n^2 \right)}}{2(R_n^2 + S_n^2)}. \quad (50)$$

Stability analyses reveal that the limit cycle with larger amplitude is stable, and the one with lower amplitude is unstable. When specialized to the moving string and only tension excitation, the results of Mockensturm et al. [1] are recovered.

The foregoing single mode analysis ignores the possibility of other modes being excited through nonlinear coupling. Figure 7 compares the nonlinear response from (50) with numerical integration of the coupled nonlinear equations from a three-term Galerkin discretization of (45). Figures 7(a) and 7(b) show that the amplitude of the first mode response is accurately predicted by single-mode analysis. There is, however, considerable energy transfer into other modes that is not captured in the single mode analysis (Figs. 7(c) and 7(d)).

Conclusions

Closed-form expressions are derived for the stability of axially moving media subjected to multifrequency parametric excitation from simultaneous tension and speed fluctuations.

1 The effects of the parametric excitations at frequencies other than the one that is the root cause of an instability are evident only in a second order perturbation. These effects, however, can be substantial. In a first-order solution, the set of primary and combination instability regions for multifrequency excitation are the superposition of the instability regions for the individual monofrequency excitations.

2 The primary instability region that one expects when an excitation frequency is twice a natural frequency shifts as a result of the multiple parametric excitations. The classical 2:1 ratio between excitation and natural frequencies no longer holds, and primary parametric instability occurs at different excitation frequencies higher or lower than $2\omega_n$ (Fig. 1).

3 Secondary resonances that are typically considered benign widen substantially when a second parametric excitation simultaneously excites a primary instability in the same mode (Fig. 3). Such conditions occur naturally when the fundamental frequency of periodic (but not sinusoidal) parametric excitation drives secondary instability and the first harmonic drives primary instability.

This provides a plausible explanation for the practically important case of a serpentine belt span oscillating at the same frequency as the engine firing frequency.

4 Instability regions for combination resonances of the sum type are significantly narrower than those for primary instability. For practical system damping and realistic excitation amplitudes, a first-order approximation appears to be sufficient. Difference type combination resonances do not occur even with multiple excitation frequencies.

5 The nonlinear response amplitude under primary instability is determined solely by the excitation causing the instability and is independent of other excitations in a first-order approximation. Transfer of energy from the unstable mode to other modes as a result of nonlinear coupling is apparent in a numerical solution (Fig. 7), though not captured in a first-order approximation.

Acknowledgment

The authors thank Mark IV Automotive/Dayco Corporation for their support of this project.

Appendix

Results in this Appendix hold for traveling strings and beams. For traveling strings ($\alpha=0$), the following relations are helpful (also see (30)):

$$C_{\bar{n}\bar{n}} = (1 - e^{-2jn\pi\gamma_0})/2, \quad D_{\bar{n}\bar{n}} = 0. \quad (51)$$

A Primary Instability Caused by Speed Fluctuation: $\Omega'_l \approx 2\omega_n$, $\varepsilon_i = 0$

$$\begin{aligned} \Omega'_l = 2\omega_n \pm \varepsilon'_l & \left| -jC_{\bar{n}\bar{n}} + 2\omega_n D_{\bar{n}\bar{n}} \right| \\ & - \left| -jC_{\bar{n}\bar{n}} + 2\omega_n D_{\bar{n}\bar{n}} \right|^2 \left[- \sum_{i=1, i \neq l}^{k'} \varepsilon_i'^2 \frac{2\omega_n}{\Omega_i'^2 - 4\omega_n^2} + \frac{\varepsilon_l'^2}{8\omega_n} \right] \\ & + \sum_{i=1}^{k'} \left(\frac{\varepsilon_i'}{2} \right)^2 |E_{nn}| \end{aligned} \quad (52)$$

B Secondary Instability Caused by Speed Fluctuation: $\Omega'_l \approx \omega_n$, $\varepsilon_i = 0$

$$\begin{aligned} \Omega'_l = \omega_n \pm \frac{\varepsilon_l'^2}{\omega_n} & \text{Im}(E_{nn}) \left| -jC_{\bar{n}\bar{n}} + \omega_n D_{\bar{n}\bar{n}} \right| \\ & - \left| -jC_{\bar{n}\bar{n}} + \omega_n D_{\bar{n}\bar{n}} \right|^2 \left[- \sum_{i=1, i \neq l}^{k'} \varepsilon_i'^2 \frac{\omega_n}{\Omega_i'^2 - 4\omega_n^2} + \frac{\varepsilon_l'^2}{3\omega_n} \right] \\ & + \sum_{i=1}^{k'} \left(\frac{\varepsilon_i'}{2} \right)^2 |E_{nn}| \end{aligned} \quad (53)$$

C Combination Instability Caused by Speed Fluctuation: $\Omega'_l \approx \omega_n + \omega_m$, $\varepsilon_i = 0$

$$\begin{aligned} \Omega'_l = \omega_n + \omega_{nn} \\ \pm \varepsilon'_l \sqrt{(-jC_{\bar{n}\bar{m}} + (\omega_n + \omega_m)D_{\bar{n}\bar{m}})(-jC_{\bar{m}\bar{n}} + (\omega_n + \omega_m)D_{\bar{m}\bar{n}})} \end{aligned} \quad (54)$$

D Primary Instability Caused by Tension and Speed Fluctuation: $\Omega_l = \Omega'_l \approx 2\omega_n$

$$\begin{aligned} \Omega_l = \Omega'_l = 2\omega_n \pm \sqrt{(\varepsilon'_l | -jC_{\bar{n}\bar{n}} + 2\omega_n D_{\bar{n}\bar{n}} |)^2 + (\varepsilon_l | E_{\bar{n}\bar{n}} |)^2} \\ - |E_{\bar{n}\bar{n}}|^2 \left[- \sum_{i=1, i \neq l}^k \varepsilon_i^2 \frac{2\omega_n}{\Omega_i^2 - 4\omega_n^2} + \frac{\varepsilon_l^2}{8\omega_n} \right] \\ - \left| -jC_{\bar{n}\bar{n}} + 2\omega_n D_{\bar{n}\bar{n}} \right|^2 \left[- \sum_{i=1, i \neq l}^{k'} \varepsilon_i'^2 \frac{2\omega_n}{\Omega_i'^2 - 4\omega_n^2} + \frac{\varepsilon_l'^2}{8\omega_n} \right] \\ + \sum_{i=1}^{k'} \left(\frac{\varepsilon_i'}{2} \right)^2 |E_{nn}| \end{aligned} \quad (55)$$

E Secondary Instability Caused by Tension and Speed Fluctuation: $\Omega_l = \Omega'_l \approx \omega_n$

$$\begin{aligned} \Omega_l = \Omega'_l = \omega_n \pm \sqrt{\left(\frac{\varepsilon_l^2}{\omega_n} \text{Im}(E_{nn}) |E_{\bar{n}\bar{n}}| \right)^2 + \left(\frac{\varepsilon_l'^2}{\omega_n} \text{Im}(-jC_{\bar{n}\bar{n}} + \omega_n D_{\bar{n}\bar{n}}) \right)^2} \\ - |E_{\bar{n}\bar{n}}|^2 \left[- \sum_{i=1, i \neq l}^k \varepsilon_i^2 \frac{\omega_n}{\Omega_i^2 - 4\omega_n^2} + \frac{\varepsilon_l^2}{3\omega_n} \right] - \left| -jC_{\bar{n}\bar{n}} + \omega_n D_{\bar{n}\bar{n}} \right|^2 \left[- \sum_{i=1, i \neq l}^{k'} \varepsilon_i'^2 \frac{\omega_n}{\Omega_i'^2 - 4\omega_n^2} + \frac{\varepsilon_l'^2}{3\omega_n} \right] + \sum_{i=1}^{k'} \left(\frac{\varepsilon_i'}{2} \right)^2 |E_{nn}| \end{aligned} \quad (56)$$

F Combination Instability Caused by Tension and Speed Fluctuation: $\Omega_l = \Omega'_l \approx \omega_n + \omega_m$

$$\Omega_l = \Omega'_l = \omega_n + \omega_m \pm \sqrt{(\varepsilon'_l)^2 (-jC_{\bar{n}\bar{m}} + (\omega_n + \omega_m)D_{\bar{n}\bar{m}})(-jC_{\bar{m}\bar{n}} + (\omega_n + \omega_m)D_{\bar{m}\bar{n}}) + (\varepsilon_l)^2 E_{\bar{n}\bar{m}} \bar{E}_{\bar{m}\bar{n}}} \quad (57)$$

References

- [1] Mockensturm, E. M., Perkins, N. C., and Ulsoy, A. G., 1996, "Stability and Limit Cycles of Parametrically Excited, Axially Moving Strings," *ASME J. Vibr. Acoust.*, **118**, July, pp. 346–351.
- [2] Pakdemirli, M., and Ulsoy, A. G., 1997, "Stability Analysis of an Axially Accelerating String," *J. Sound Vib.*, **203**, No. 5, pp. 815–832.
- [3] Mahalingam, S., 1957, "Transverse Vibrations of Power Transmission Chains," *Br. J. Appl. Phys.*, **8**, pp. 145–148.
- [4] Mote, C. D. Jr., 1965, "A Study of Band Saw Vibrations," *J. Franklin Inst.*, **279**, No. 6, pp. 430–444.
- [5] Mote, C. D. Jr., 1968, "Dynamic Stability of an Axially Moving Band," *J. Franklin Inst.*, **285**, No. 5, pp. 329–346.
- [6] Naguleswaran, S., and Williams, C. J. H., 1968, "Lateral Vibrations of Band Saw Blades, Pulley Belts, and the Like," *Int. J. Mech. Sci.*, **10**, pp. 239–250.
- [7] Asokanathan, S., and Ariaratnam, S., 1994, "Flexural Instabilities in Axially Moving Bands," *ASME J. Vibr. Acoust.*, **116**, No. 3, pp. 275–279.

- [8] Oz, H. R., Pakdemirli, M., and Ozkaya, E., 1998, "Transition Behavior From String to Beam for an Axially Accelerating Material," *J. Sound Vib.*, **215**, No. 3, pp. 571–576.
- [9] Chakraborty, G., and Mallik, A. K., 1998, "Parametrically Excited Non-linear Traveling Beams With and Without External Forcing," *Nonlinear Dyn.*, **17**, No. 4, pp. 301–324.
- [10] Ulsoy, A. G., Whitesell, J. E., and Hooven, M. D., 1985, "Design of Belt-Tensioner Systems for Dynamic Stability," *ASME J. Vibr. Acoust.*, **107**, No. 3, pp. 282–290.
- [11] Nayfeh, A. H., and Mook, D. T., 1979, *Nonlinear Oscillations*, John Wiley and Sons, New York.
- [12] Wickert, J. A., and Mote, C. D. Jr., 1990, "Classical Vibration Analysis of Axially Moving Continua," *ASME J. Appl. Mech.*, **57**, pp. 738–744.
- [13] McLachlan, N. W., 1947, *Theory and Applications of Mathieu Functions*, Oxford University Press, New York.